Journal of Alloys and Compounds 509 (2011) 1563–1566

Contents lists available at ScienceDirect

Journal of Alloys and Compounds

journal homepage: www.elsevier.com/locate/jallcom

Microstructure evolution of the undercooled Co–Ni–Ga magnetic shape memory alloy

Junzheng Li, Jianguo Li*

School of Materials Science and Engineering, Shanghai Jiao Tong University, Shanghai 200240, PR China

ARTICLE INFO

Article history:
Received 6 October 2010
Accepted 21 October 2010
Available online 29 October 2010

Keywords:
Undercooling
Sub-grain
Co–Ni–Ga
Magnetic shape memory alloy

ABSTRACT

Microstructure evolution of the martensite $Co_{50}Ni_{22}Ga_{28}$ magnetic shape memory alloy was investigated by the method of glass fluxing combined with superheating cycling. A maximum bulk undercooling of 220 K is achieved and a mass of sub-grains are introduced by the undercooling. A number of dislocations and large internal stress, due to the undercooling rapid solidification, give rise to the production of sub-grains during the recovery process. These sub-grains, as well as martensite variants, are remarkably refined with the increase of undercooling. The recrystallization and growth of sub-grains during the following annealing are also discussed.

1. Introduction

Since the first report came out on the large magnetic field-induced strain in the Ni_2MnGa ferromagnetic shape memory alloy (FSMA) [1], much progress has been made in studies of FSMAs. Several systems including Fe–Pd [2], Fe_3Pt [3], Ni–Fe–Ga [4], Co–Ni–Al [5], Co–Ni–Ga [6–12] and so on have been proposed as new FSMAs, among which the Co–Ni–Ga alloy attracts considerable attention owing to its magnetic-controlled two-way shape memory effect [8], high martensitic transformation temperatures [9] and high ductility [7]. Sato et al. discovered that the textured Co–Ni–Ga alloy prepared by melt-spinning rapid solidification exhibited large magnetic-field-induced strain (MFIS) [10]. Our previous research into the Co_2NiGa alloy treated by undercooling rapid solidification found that the γ phase was significantly refined with undercooling (ΔT), which would improve the alloy ductility [11]. Thus it can be seen that rapid solidification, especially for the undercooling rapid solidification, is a promising method to improve the alloy microstructure and in turn enhances its properties.

By means of the undercooling rapid solidification, the martensitic transformation temperature and crystal structure could be changed in the single-phase $Co_{46}Ni_{27}Ga_{27}$ alloy [12], which was attributed to the effect of large internal stress introduced in rapid solidification. Dragnevski et al. [13] found in the undercooled pure Cu sample a high density of sub-grains, which were deemed to result from some redistribution of line defects introduced by rapid solidification. A similar phenomenon was also noticed in the undercooled DD3 single crystal superalloy [14]. These results suggest that large internal stress introduced by undercooling can induce sub-grains, which will inevitably affect the MFIS for FSMAs. This finding is interesting because sub-grains are usually reported to be introduced in high deformative materials by thermo-mechanical processing [15–20], and there are few studies concerning sub-grains introduced in FSMAs, let alone particular discussions on the relationship between sub-grains and undercooling. In this paper, we carried out a systemic study on the martensite $Co_{50}Ni_{22}Ga_{28}$ alloy, which was treated by glass fluxing combined with superheating cycling and following annealing. The microstructure evolution under different undercoolings, especially the occurrence of sub-grains, was investigated.

2. Experimental

Ingots of the nominal $Co_{50}Ni_{22}Ga_{28}$ alloy were prepared by arc-melting under an argon atmosphere. They were melted four times and homogenized in a vacuum heat treatment furnace at 1273 K for 48 h. Samples with the mass in 1.5 g were cut from the ingots for the undercooling experiments which were performed in a high frequency induction unit under an argon atmosphere. The method of glass fluxing combined with superheating cycling was used to achieve a reasonable large undercooling. The fluxed glass, consisting of 70 wt.% $Na_2B_4O_7$, 30 wt.% NaSiCa, was employed as the denucleating agent. The undercooling experimental apparatus and experimental process were described in our previous report [11]. Some undercooled samples underwent annealing at 1073 K for 4 h, followed by furnace cooling.

The optical microscopy (Neo-plot1 OM), the scanning electron microscopy (SEM520 SEM) and the transmission electron microscopy (JEM-2100 TEM) were used to examine the microstructure. Composition was determined by energy dispersion X-ray spectroscopy (EDS). The thin foils for TEM were electrochemically polished by the twin jet method in a solution of 20% HNO_3 and residual ethanol.

* Corresponding author. Tel.: +86 21 54744119; fax: +86 21 54744119.
E-mail addresses: junzhengli@sjtu.edu.cn (J. Li), lijg@sjtu.edu.cn (J. Li).

0925-8388/$ – see front matter © 2010 Elsevier B.V. All rights reserved.
doi:10.1016/j.jallcom.2010.10.080

Table 1
Chemical composition of the $Co_{50}Ni_{22}Ga_{28}$ alloy measured by EDS.

Alloy	Chemical composition (at.%) (±0.05%)		
	Co	Ni	Ga
As-cast	49.67	22.27	28.07
ΔT = 220 K	49.14	22.25	28.60

3. Results and discussion

A maximum undercooling for the $Co_{50}Ni_{22}Ga_{28}$ alloy reaches 220 K. The EDS analysis of rapidly solidified samples with different undercoolings confirms that no chemical reaction occurred between the alloy melt and the denucleating glass. Accordingly, the alloy composition remains almost unchanged by undercooling. (Table 1)

The typical microstructure of the $Co_{50}Ni_{22}Ga_{28}$ alloy with a wide range of undercoolings from 72 K to 220 K is shown in Fig. 1. It can be seen that the samples at various undercoolings possess single martensite phase, but the morphologies of martensite change observably with the undercooling increasing. When the undercooling is about 72 K, there is a single variant with the width of about 80 μm (Fig. 1a). The variant width dramatically declines and its boundary becomes indistinct with the increase of undercooling (Fig. 1b–d). When the undercooling rises to 220 K, the variant width decreases to 30 μm. Besides, it is observed that at the undercooling of 72 K a mass of equixed sub-grains, which are about 150 μm in size with indistinct sub-boundaries (Fig. 1a), are introduced in the martensite variant. Such sub-grains are also found in the undercooled pure Cu sample and DD3 superalloy [13,14]. These sub-grains are obviously refined and their sub-boundaries become more and more distinct with the undercooling increasing (Fig. 1b–d). When the undercooling reaches about 220 K, the high undercooling introduces a well-developed network of both a high angle of boundaries and a low angle of sub-boundaries (Fig. 1d).

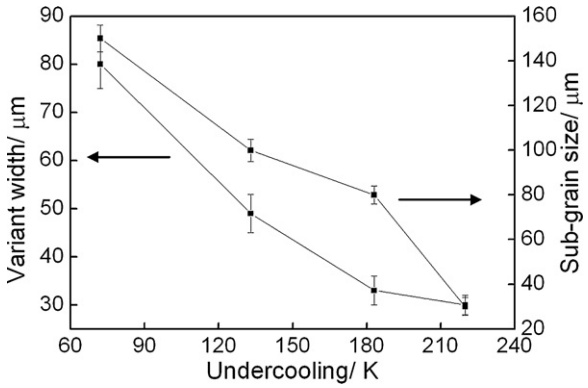

Fig. 2. Martensite variant width and sub-grain size as functions of the undercooling.

Fig. 2 shows the martensite variant width and sub-grain size as functions of the undercooling. It can be seen that both the variant and the sub-grain are remarkably refined by undercooling. While the martensite variant width decreases from 80 μm at undercooling of 72 K to 30 μm at 220 K, the sub-grain size also decreases from 150 μm to 50 μm. Ma et al. [21] discovered that the grain size was considerably refined in the undercooled $Fe_{80}Ga_{20}$ alloy. Our previous study found that the size of γ phase was reduced with the undercooling increasing in the Co_2NiGa alloy [11]. Both of the results were well explained by the classical nucleation theory [22], which points out that the higher undercooling can increase the nucleation rate and decrease the critical activation energy. Since the martensite transformation is the process of martensite nucleation and growth, the refinement of martensite variants can also be explained by the classical nucleation theory. High undercooling increases the number of vacancy and dislocation, hence generates an internal stress field [23]. These defects act as the nucleation core and increase with the undercooling; the internal stress decreases the activation energy and also increases with the undercooling.

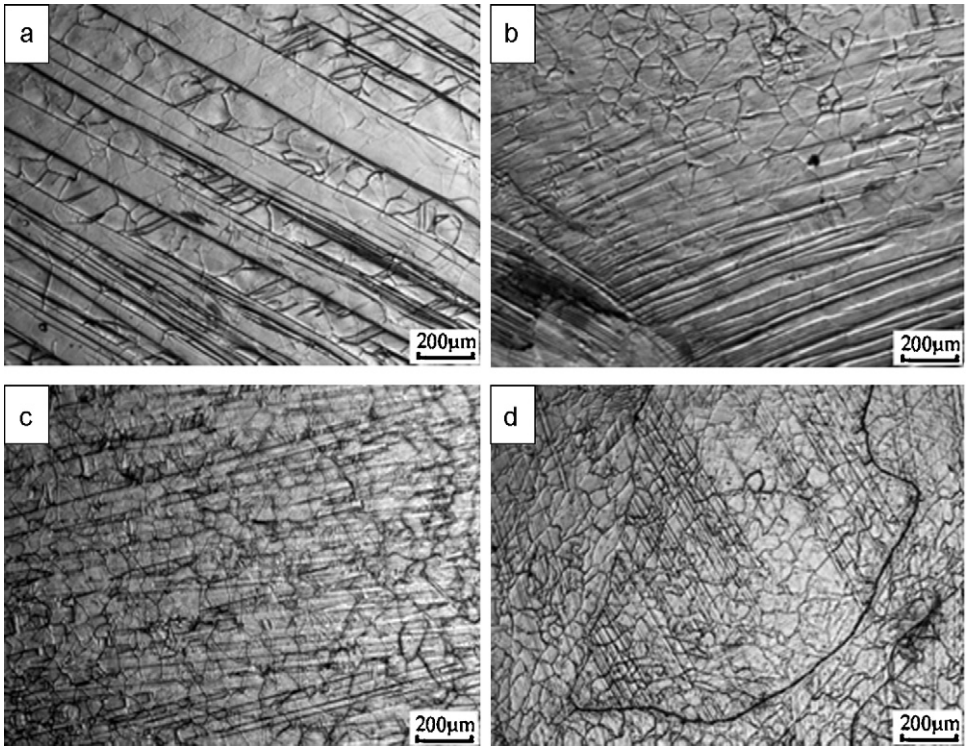

Fig. 1. Microstructure of the $Co_{50}Ni_{22}Ga_{28}$ alloy undercooled by (a) 72 K, (b) 133 K, (c) 183 K, (d) 220 K.

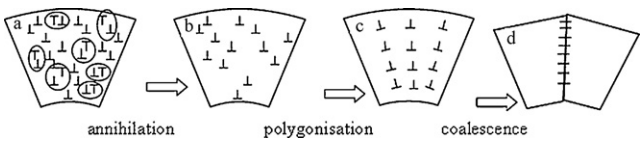

Fig. 3. Schematic of the micromechanism of sub-grain formation during recovery.

Thus, the nucleation rate rises and the critical activation energy declines with the undercooling increasing, which are propitious for the martensite transformation and the martensite variant refinement.

As is mentioned in the literature [15–20], sub-grains usually appear in high deformative metal materials. Studies on thermo-mechanical processing have proved that deformation structures store high internal stress and release the stored energy by recovery, recrystallization and eventual grain growth during the following annealing [15–17]. These three 'softening' processes involve a set of micromechanisms for the motion and annihilation of point defects, dislocations and boundaries [18–20]. That fine sub-grains in the undercooled Co–Ni–Ga alloy are induced by undercooling rapid solidification is similar to what happened to the thermo-mechanical processing. Fig. 3 shows the schematic of the micromechanism of sub-grain formation during recovery. At the rapid growth stage after recalescence, the sudden volume contraction and the cavity collapse of undercooled liquid would result in a large number of vacancies, interstitials and dislocations (Fig. 3a), the amounts of which increase with the undercooling and thus generate an internal stress field [23]. Also, higher undercooling would introduce more defects and larger internal stress. With the sample cooling down, its internal stress gradually increases and induces recovery. Small amounts of dislocations, which are closely spaced dislocations of opposite sign (encircled pairs), climb and/or cross slip to annihilate (Fig. 3a and b). Meanwhile, these point defects (vacancies and interstitials) would be annihilated by diffusion of dislocations. The remaining free and random dislocations rearrange into dislocation walls, lead to polygonization (Fig. 3c), and eventually reorganize into sub-boundaries (Fig. 3d). The refinement of sub-grains is due to the higher undercooling, which results in higher solidification velocity and inevitably causes more dislocations, in turn increasing the number of sub-grains, i.e., refining sub-grains.

To further investigate the possible rearrangement of dislocations, higher magnification of optical micrograph and TEM analysis were carried out on the alloy undercooled by 220 K (Fig. 4). The optical micrograph shows that a large number of sub-grains are in the size of 50 μm and appear as polygon rather than exact rotundity (Fig. 4a), which demonstrates that the dislocations rearrange into dislocation walls and result in polygonization as we assumed. From the TEM dark field image of the sample (Fig. 4b), it is evident that dislocations in the martensite variants have realigned into walls, which stick together to form a fine array of sub-boundaries.

In order to achieve a systematic micromechanism on sub-grains induced by undercooling, the recrystallization and the growth of sub-grains during the following annealing were also investigated. Fig. 5 shows the microstructure of the $Co_{50}Ni_{22}Ga_{28}$ alloy undercooled by 220 K annealed at 1073 K for 4 h. It is found that the grains have obviously grown up with sub-grains disappearing (Fig. 5a), which demonstrates the recrystallization of sub-grains during the annealing process. Meanwhile, the martensite variant grew up and

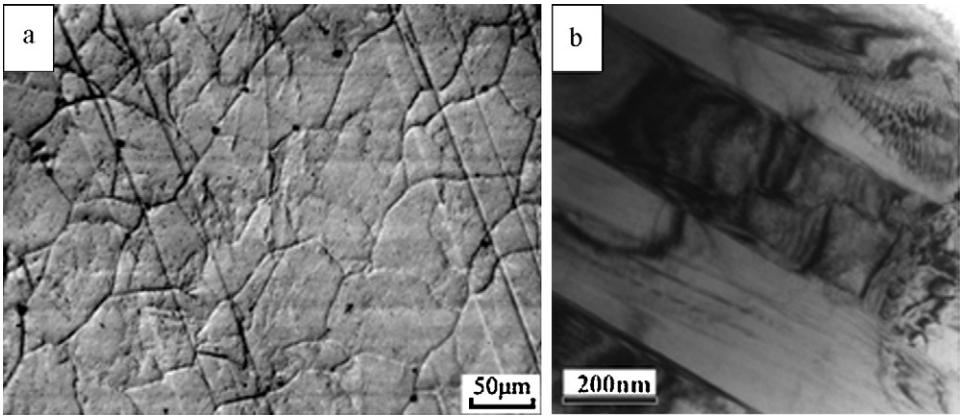

Fig. 4. Microstructure of the $Co_{50}Ni_{22}Ga_{28}$ alloy with undercooling of 220 K: (a) optical micrograph at higher magnification, and (b) TEM dark field image of several fine dislocation walls.

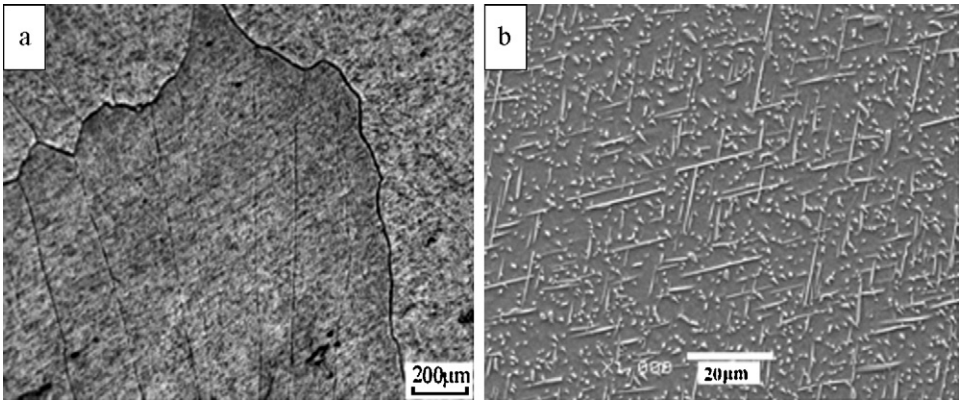

Fig. 5. Microstructure of the $Co_{50}Ni_{22}Ga_{28}$ alloy with undercooling of 220 K annealed at 1073 K for 4 h (a), SEM with higher magnification of an amount of precipitate.

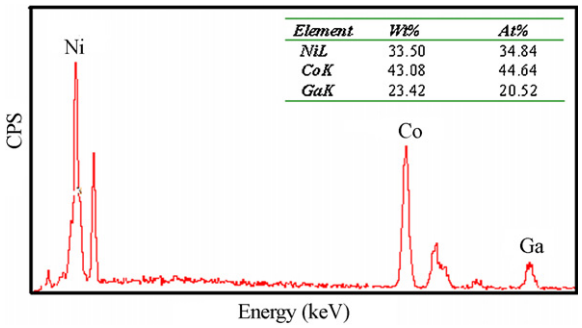

Fig. 6. EDS measured from the precipitate.

its width reached 200 μm. The martensite variants traverse the sub-boundaries (Figs. 1 and 4a) but stop at the boundaries (Fig. 5a), which may be attributed to the fact that the sub-boundaries are low-energy configurations but the boundaries are high-energy ones. The phenomenon can also prove that high undercooling indeed induces a mass of sub-grains instead of the refinement of grains. The SEM image shows an amount of fine precipitate dispersing uniformly in martensite matrix (Fig. 5b), whose morphology exhibits a needle-like or particle structure. According to the EDS curve of the precipitate in Fig. 6, the atomic ratio of (Co + Ni):Ga is 3:1. Liu et al. have carried a systematic study on the precipitate of the annealed Co–Ni–Ga alloy and found similar precipitate [24], which was considered as low-temperature equilibrium ordered γ′ phase.

4. Conclusions

(1) By using glass fluxing combined with superheating cycling method, the $Co_{50}Ni_{22}Ga_{28}$ magnetic shape memory alloy achieves 220 K maximum undercooling with no composition changed.
(2) The martensite variant is remarkably refined with the increase of undercooling. A mass of sub-grains are not only induced but also refined with undercooling.
(3) The micromechanism of sub-grains induced by undercooling rapid solidification is discussed. A number of dislocations and large internal stress give rise to the occurrence of sub-grains during the recovery process.
(4) The sub-grains recrystallize and grow into coarse grains during the annealing process, where an amount of fine needle-like γ′ phase precipitates.

Acknowledgements

The authors express their appreciation for the financial support of the National Natural Science Foundation (No. 50671068) and the Shanghai Natural Science Foundation (No. 10ZR1416200) of China.

References

[1] K. Ullakko, J. Mater. Eng. Perform. 5 (1996) 405.
[2] R.D. James, M. Wuttig, Philos. Mag. A 77 (1998) 1273.
[3] T. Kakeshita, T. Takeuchi, T. Fukuda, M. Tsujiguchi, T. Saburi, R. Oshima, S. Muto, Appl. Phys. Lett. 77 (2000) 1502.
[4] K. Oikawa, T. Ota, Y. Sutou, T. Ohmori, R. Kainuma, K. Ishida, Mater. Trans. 43 (2002) 2360.
[5] J. Liu, J.G. Li, Mater. Sci. Eng. A 454–455 (2007) 423.
[6] M. Wutting, J. Li, C. Craciunescu, Scripta Mater. 44 (2001) 2393.
[7] K. Oikawa, T. Ota, F. Gejima, T. Ohmori, R. Kainuma, K. Ishida, Mater. Trans. 42 (2001) 2472.
[8] Y.X. Li, H.Y. Liu, F.B. Meng, L.Q. Yan, G.D. Liu, X.F. Dai, M. Zhang, Z.H. Liu, J.L. Chen, G.H. Wu, Appl. Phys. Lett. 84 (2004) 3594.
[9] J. Liu, H.X. Zheng, M.X. Xia, Y.L. Huang, J.G. Li, Scripta Mater. 52 (2005) 935.
[10] M. Sato, T. Okazaki, Y. Furuya, M. Wuttig, Mater. Trans. 44 (2003) 372.
[11] J.Z. Li, J. Liu, M.X. Zhang, J.G. Li, J. Alloys Compd. 499 (2010) 39.
[12] J. Liu, Y.Q. Huo, H.X. Zheng, J.G. Li, Mater. Lett. 60 (2006) 1693.
[13] K.I. Dragnevski, R.F. Cochrane, A.M. Mullis, Mater. Sci. Eng. A 375–377 (2004) 479.
[14] F. Liu, G.C. Yang, X.F. Guo, Mater. Sci. Eng. A 311 (2001) 54.
[15] S. Straub, W. Blum, H.J. Maier, T. Ungár, A. Borbély, H. Renner, Acta Mater. 44 (1996) 4337.
[16] B. Kockar, I. Karaman, J.I. Kim, Y.I. Chumlyakov, J. Sharp, C.J. Yu, Acta Mater. 56 (2008) 3630.
[17] B. Verlinden, J. Driver, I. Samajdar, R.D. Doherty, Thermo-Mechanical Processing of Metallic Materials, Elsevier, 2007, pp. 85–105.
[18] W. Blum, Y.J. Li, K. Durst, Acta Mater. 57 (2009) 5207.
[19] Y. Huang, F.J. Humphreys, Acta Mater. 45 (1997) 4491.
[20] Y. Huang, F.J. Humphreys, Mater. Charact. 47 (2001) 235.
[21] W.Z. Ma, H.X. Zheng, M.X. Xia, J.G. Li, J. Alloys Compd. 379 (2004) 188.
[22] D. Turnbull, Contemp. Phys. 10 (1969) 473.
[23] G.L. Powell, L.M. Hogan, Trans. Metall. Soc. AIME 245 (1969) 407.
[24] J. Liu, H. Xie, Y.Q. Huo, H.X. Zheng, J.G. Li, J. Alloys Compd. 420 (2006) 145.